Ecohydrology

WILEY

RESEARCH ARTICLE OPEN ACCESS

Variation in Water-Use Strategies of *Prosopis velutina* in Southern Arizona

Collin Gillespie[1] | Gita Bodner[2] | Russell L. Scott[3] | Jia Hu[1]

[1]School of Natural Resources and the Environment, University of Arizona, Tucson, Arizona, USA | [2]The Nature Conservancy, Tucson, Arizona, USA | [3]Southwest Watershed Research Center, USDA-ARS, Tucson, Arizona, USA

Correspondence: Collin Gillespie (collin.gillespie@gmail.com)

Received: 27 January 2025 | **Revised:** 7 January 2026 | **Accepted:** 24 January 2026

Keywords: leaf water potential | mesquite | plant water use | *Prosopis velutina* | source water | stable isotopes

ABSTRACT

In semi-arid regions of the United States, mesquite trees are widely distributed across the landscape and play a pivotal ecological role, influencing hydrological processes and contributing to biodiversity. This is especially true in riparian areas, where understanding the adaptive water-use strategies of facultative phreatophytes is essential to understanding ecohydrology in this region and in similar dryland ecosystems worldwide. This study investigated the water-use strategies of mesquite trees (*Prosopis velutina*) located in the floodplain of the San Pedro River in southern Arizona, USA across two contrasting water years, a dry winter/wet summer (2022) versus a wet winter/dry summer (2023). We explored the impact of age, size and density of mesquite stands (characterized as mature trees, dense young thicket and thinned young thicket) to understand how these trees access both deep (groundwater) and shallow soil moisture (recent precipitation). Across stand types, trees opportunistically used both deep and shallow source water, a strategy that is consistent in woody plants that grow with a bimodal precipitation regime. That relatively young thickets show similar strategies to mature bosques demonstrates the potential for rapid restoration to bosque form and function. We also examined leaf water potential to assess seasonal water stress between the two water years and found that despite the summer precipitation in 2023 being 111% lower than in 2022, summer leaf water potential had similar dynamics. This unexpected result leads us to posit that the higher winter precipitation in 2023 compared to 2022 (91% higher) helped to buffer the trees in 2023 from water stress, even during a drier summer. This suggests that winter precipitation (deeper in the soil profile) remains an important water source for trees, even in dryland regions where surface water along riparian areas is readily available.

1 | Introduction

Velvet mesquite (*P. velutina*) is an iconic species that has evolved over millennia to adapt to the harsh conditions of the Sonoran and Chihuahuan Deserts (Brown 1982; Scott, Huxman, et al. 2006). Their dimorphic root system and drought-tolerant physiology are often celebrated as ecological assets allowing them to survive and even flourish where few other trees can (Nilsen et al. 1981). As facultative phreatophytes, they can be found in diverse habitats including upland desert-scrub, semi-arid grasslands (Archer et al. 1988; Snyder and Williams 2000), ephemeral washes and river floodplains (Stromberg 1993); form and function can be very different in each of these settings. Encroachment or expansion of mesquites is a widespread and much-studied phenomenon in semi-arid grassland settings (McClaran and Van Devender 1995; Archer et al. 2017), however, prevalence and density of mesquites in other settings can be stable or even declining.

River terrace settings are the focus of this study. Expansive, dense stands of large mesquite trees called *bosques* were once the most abundant type of riparian woodlands in the southwestern United States, but now they are increasingly rare and face many threats such as groundwater pumping, land clearing

and competition from invasive species (Stromberg et al. 1992; Stromberg et al. 1993). However, younger mesquite stands, often growing in dense thickets as a result of farmland left fallow on the same near-stream terraces that may have historically held bosques, frequently receive scrutiny over concern about the impact these trees may have on groundwater levels. With few studies done in these thickets, there is a gap in our understanding of how water use in these younger thickets compares with mature mesquite bosque in similar settings, or with the much more widespread mesquite stands in drier upland settings.

Mesquite are well known for their ability to access soil water at a wide range of depths and can be an important contributor to evapotranspiration in this region. Previous work examining the water-use patterns of velvet mesquite along with co-occurring semi-arid riparian phreatophytes found that these species use significant quantities of groundwater (Sabathier et al. 2021; Scott, Goodrich, et al. 2006; Snyder and Williams 2007) and that velvet mesquite redistributed water vertically and laterally through their roots, even during periods of crown dormancy (Hultine et al. 2004). Snyder and Williams (2000) found stands of velvet mesquite growing along the San Pedro River used both groundwater and shallow soil moisture, but in different proportions depending on the surface flow regime (an indicator of groundwater depths and fluctuations) in the nearest reach of the river. However, stand characteristics such as tree age, stand density, depth to groundwater and other factors may have significant impacts on plant water-use strategies but have not been thoroughly explored. While velvet mesquite seedlings prioritize root growth over canopy growth (Stromberg 1993), how this early root growth translates into source water use as trees age is not clear. Stand density may be an important factor impacting water-use patterns as it can be directly related to competition, which may affect water availability (Castagneri et al. 2022), but it is unclear how water-use strategies specifically in mesquite respond to changes in stand density. By tracking source water use over time using stable isotope analysis, studies have examined where other tree species source water from in the soil column, how this varies seasonally based on changes in soil moisture availability and how this varies between stands of different ages, densities and depths to groundwater (Allen et al. 2019; Ehleringer and Dawson 1992; Lin et al. 1996; Snyder and Williams 2000). This knowledge lends itself to more accurate assessments of catchment-level water budgets in the semi-arid and arid basins where this species is found (Scott et al. 2008). Such an exploration may also yield valuable insight into the restoration potential of riparian vegetation and could help to corroborate predictions that large, mature mesquite trees could eventually degrade to the smaller shrub forms typical of upland areas in the face of climatic shifts and declining water tables (Stromberg 2001; Stromberg et al. 1993).

Groundwater decline in southern Arizona has been a problem since the 1940s (Conway 2016), and the resultant impacts on streamflow have been seen across Arizona, including in the riparian areas where mesquite bosques are found (Haney 2005). While it has been shown that increased woody plant cover, especially in areas where groundwater is shallow enough to be accessible to plants, can lead to greater evapotranspiration and potentially decreased streamflow (Huxman et al. 2005; O'Keefe et al. 2020; Scott, Goodrich, et al. 2006), there is a continued assumption that removal of woody plants such as mesquite can lead to increased streamflow and, as a result, the practice continues (Archer and Predick 2014; Gungle et al. 2016; Keen et al. 2022; Wilcox 2002). However, studies examining the effects of woody plant removal, including mesquite, both in upland and riparian zones, have not shown substantive increases in streamflow (Keen et al. 2022; Dodds et al. 2023; Wilcox 2002; Wilcox et al. 2006). Mesquite stands of greater density are also said to be of higher concern regarding changes in habitat and erosion dynamics, particularly in upland areas (Wilcox 2002; Wilcox et al. 2006), but the importance of stand density in riparian areas needs further study.

To refine our understanding of the variations in water-use strategies among different-aged stands of riparian mesquite, including a mature stand (i.e., bosque), a young dense thicket and a young and recently thinned thicket, we conducted this study over two different water years. Southwestern Arizona has a bimodal precipitation regime, with about half of the precipitation delivered during the winter and the other half delivered during the summer (Adams and Comrie 1997). Previous studies have found mesquite trees to be highly sensitive to the summer rains that are delivered by the North American Monsoon system (Potts et al. 2008; Scott et al.2008). However, many of the perennial streams across the southwestern United States are fed by groundwater, which reflects disproportionately more winter precipitation than summer precipitation (Eastoe and Towne 2018). Specifically, we addressed three main questions: (1) Along a riparian corridor, do different *P. velutina* stands (varying in stand density and age) access and use different sources of water? (2) How do the patterns of tree source water use vary throughout the year? (3) How do potential differences in water access and use impact tree water stress?

2 | Methods

2.1 | Site Description

The research site is located at Middle San Pedro River Preserve (also known as the Three Links Farm) (32.1880, −110.3012), a Nature Conservancy preserve in southern Arizona. The property is bisected by the San Pedro River, which has intermittent flow in this reach only during and shortly after periods of precipitation, usually between June and September; during our study period, the river also experienced infrequent flows from October to January, depending on rain events. Three Links was once an active farm growing alfalfa, wheat and milo and was purchased by The Nature Conservancy (TNC) in 2002 (Figure 1). The property has had periods of cattle-grazing before 2002 and some intermittent grazing since. An approximately 324-ac area on the East side of the San Pedro was cleared for farming in the 1950s, and then fallowed in 2002 and allowed to self-recruit. In that time, it grew in with *P. velutina* (Velvet mesquite), which is densest in the Southeastern part of the now fallow field and increasingly thin further northwest. Trees in this area have heights of 5–7 m, and while most trees are multistemmed at ground level, some single stemmed trees have a DBH (diameter at breast height) as large as ~25 cm. There is also an understory consisting of annual grasses, forbs and shrubs, but little to no other tree species.

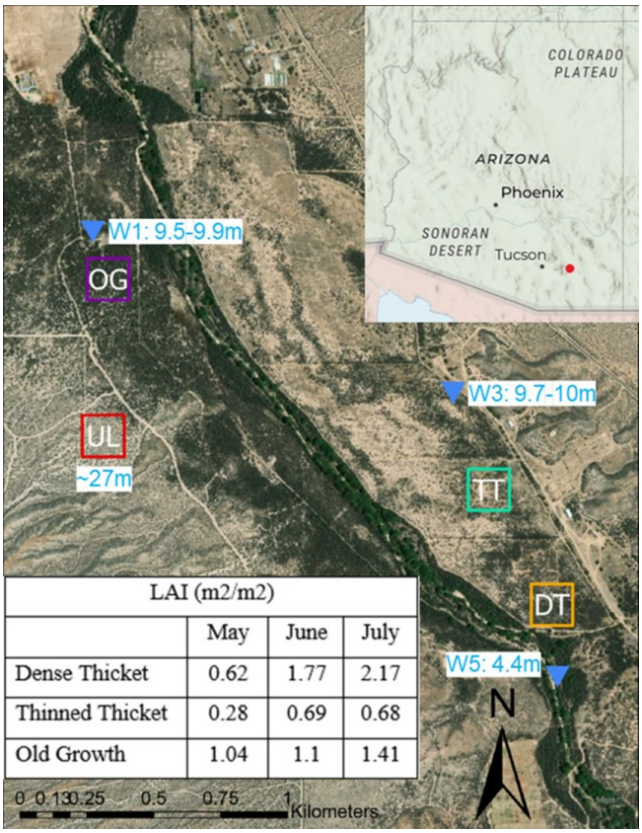

LAI (m2/m2)			
	May	June	July
Dense Thicket	0.62	1.77	2.17
Thinned Thicket	0.28	0.69	0.68
Old Growth	1.04	1.1	1.41

FIGURE 1 | Map of Three Links Farm, located in southern Arizona. Squares indicate study plots. DT, dense young thicket; OG, old-growth mature bosque; TT, thinned young thicket; UL, upland. Blue triangle points and text indicate depth to groundwater at the respective well sites. The inset table displays Leaf Area Index (LAI) measured at the indicated test plots.

The soils in this area are characterized as sandy loam. The west side of the river has an older mesquite bosque where the trees were much larger than those on the east side of the river, reaching heights of 10–13 m. Some of the largest trees have a DBH of up to 62 cm, which could indicate ages of ~125 years or more (Gavin 1973; Minckley and Clark 1984). The understory here is more diverse, and there are some other tree species present such as *Celtis reticulata*, *Vachellia constricta* and *Sapindus saponaria*. The area immediately adjacent to the river also hosts *Populus fremontii* and *Tamarix ramosissima,* though these do not extend far beyond the riverbanks. We consider the study area to be riparian insofar as it is near a stream and the depth to groundwater ranges from 4.4 to 10 m between tested wells (Figure 1).

The climate in this area is characterized as semi-arid. At a nearby weather station in Cascabel, AZ, annual precipitation averaged 342 ± 75.5 mm since 2011 (Arizona State Climate Office 2022). This region typically experiences two primary periods of precipitation. During the period of record, there was a season of convective precipitation from the North America Monsoon from June–September during which ~66% of the annual precipitation fell, with much of the rest occurring mainly during the winter months of November–February as orographic rain coming from Pacific fronts during which ~21% of the annual precipitation fell. During the warmest time of the year, June–August, daily average highs reached 37.1°C ± 1.8°C, while lows dipped to 17.2°C ± 2.8°C. The coldest period from November–February had highs of 19.6°C ± 2.9°C and lows of −0.6°C ± 2.6°C (Arizona State Climate Office 2022). Riparian sites and vegetation that are supported by groundwater typically have rates of ET that exceed local precipitation, especially in semi-arid areas where groundwater is often recharged nonlocally along mountain fronts or from flow events in the river (Kennedy and Gungle 2010).

Several nonpumped wells on the property were measured quarterly for depth to groundwater. The wells closest to the study areas were the W1, W3 and W5 wells. In 2022, the W1 well had a depth to groundwater of 9.5 m in spring and 9.9 m in summer. The W3 well had a depth to groundwater of 9.7 m in spring and 10 m in summer. The W5 well had a depth to groundwater of 4.4 m in spring and summer. The UL plot likely had a depth to groundwater of at least 27 m as it was approximately 16 m higher in elevation than the nearest well that averaged 11 m depth to groundwater.

2.2 | Study Design

We established four, 2.43-ha test plots to represent the four main mesquite stand characteristics: An old-growth mesquite bosque (OG) close to the San Pedro River, a younger dense thicket plot (DT) close to the river, a different young thicket area close to the river that was less dense due to different starting conditions but was also given a thinning treatment (TT), and one nonriparian stand in an upland area farther from the river at higher elevation (UL). We included the UL plot to provide a contrast to the sites close to the river, given that ground water depth was deeper in the UL plot and may be out of reach of mesquite roots. The thinning treatment administered in late February of 2022 consisted of removing approximately 25% of the mesquite stems via cutting and the use of Imazapyr, an herbicide that was carefully applied to the stumps to prevent regrowth. This was part of a larger study that looked at additional vegetation and habitat parameters across a larger set of plots; details can be found in Bodner (2025).

We measured local meteorological and soil conditions at all of the test plots except for the upland plot (UL) using Zentra ZL6 Basic Data Loggers (METER Environment Inc., Pullman, WA), which recorded air temperature, relative humidity and atmospheric pressure (Atmos 14, METER Environment Inc., Pullman, WA), soil temperature and soil volumetric water content (VWC) at 10 and 30 cm depths (Teros 11, METER Environment Inc., Pullman, WA) and precipitation (ECRN-100, METER Environment Inc., Pullman, WA). These data were logged at 1-h intervals from May 2021 until August of 2023. We calculated vapour pressure deficit (VPD; kPa) using air temperature and relative humidity.

2.3 | Leaf Area Index

We measured leaf area index (LAI) between May when trees were just beginning to leaf out and July of 2022 when trees had fully leafed out using a LAI-2000 Plant Canopy analyser

(LI-COR Biosciences, Lincoln, NE) to get an estimate of tree canopy density in our study plots. This device measured how sunlight was dispersed as it passed through the canopy to determine LAI, which defines leaf area per unit ground surface area. We did this to compare the timing and rate of leaf out between our study plots and to roughly quantify the canopy density when the trees were fully foliated (Figure 1). At each site, from the meteorological station, we walked 100 m in each cardinal direction, taking LAI measurements every 20 m. We averaged the measurements from all four directions for a site LAI value. It should be noted that the LAI value does not distinguish between leaves and branches so it can also be thought of as plant area index.

2.4 | Tree Source Water

We selected nine trees of varying sizes (5–62.5-cm DBH) at each of the plots from which we collected stem samples every 4–8 weeks. Stems of approximately 0.25 cm in diameter were cut and sealed with parafilm in glass vials to be used for subsequent δ^2H_{xylem} (xylem hydrogen isotope) and $\delta^{18}O_{xylem}$ (xylem oxygen isotope) analysis (Brunel et al. 1995; Snyder and Williams 2000). We dug shallow soil pits at each plot and collected soil samples at 5, 20 and 50 cm depth for soil-water extraction. Both the stem samples and soil samples were kept cool until they could be stored in our lab freezer and later extracted using cryogenic water distillation (Ehleringer et al. 2000). We also used two rain gauges near the TT with a 2-cm layer of mineral oil to prevent evaporation and, from these, collected precipitation samples that were then sealed in parafilmed glass vials and refrigerated until analysis. Additionally, we drew water samples from wells around the property to compare tree water to the groundwater isotopic signature. We used activated charcoal to filter the extracted stem samples according to West et al. (2010) to remove any potential impact from organic contamination. All the samples were analysed using a Picarro L2130i oxygen and hydrogen isotope analyser for $\delta^{18}O$ and δ^2H. The analyser advertises a precision of $\delta^{18}O$—0.025‰ and δ^2H—0.1‰. We used the Picarro ChemCorrect software to check for interference from plant organics in the xylem samples. In previous studies in this region, Chen et al. (2020) found up to a 10‰ fractionation offset in δ^2H_{xylem} during water uptake through the roots in mesquite. As a result, we have included a −9‰ correction to all the δ^2H_{xylem} results in accordance with the findings in Ellsworth and Williams (2007) for mesquite.

2.5 | Leaf Water Potential and Evaporation

Between May and October for each year, we measured leaf water potential (Ψ_{leaf}) every 3 to 6 weeks to compare seasonal water stress between tree size classes and between test plots. We used a Scholander pressure chamber (PMS Instrument, Albany, OR) to measure Ψ_{leaf} from healthy stems taken at chest level or the lowest possible height from the nine trees at each plot both at predawn (Ψ_{PD}) and at midday (Ψ_{MD}). Stems were taken from the same area of each tree, which was usually partially shaded from the overlying canopy at midday. For the predawn measurements, we collected foliated cuttings, stored them in sealed plastic bags and placed them in a cooler until we were able to measure them all in quick succession. For the midday measurements, we measured each cutting immediately after it was collected, all within a 2-h period.

We used remotely sensed monthly evapotranspiration (ET) estimates based on the Google Earth Engine Surface Energy Balance Algorithm for Land (geeSEBAL v0.2.2) model to compare ET between our study plots (OpenET—User Platform n.d.) for the 2019–2023 water years. We were interested to see if the thinning treatment administered to the TT plot would have a noticeable impact on ET, as well as examine how the DT and TT would compare to the OG stand and the contrasting nonriparian UL stand.

The geeSEBAL (Bastiaanssen, Menenti et al., 1998; Bastiaanssen, Pelgrum et al., 1998) is an open-sourced approach that uses satellite measurements of surface temperature and reflectance, land surface characteristics and weather to calculate the surface energy budget. SEBAL estimates ET (or Latent Heat Flux, LE) from the energy balance equation (ET = Rn—G—H), where Rn, G and H are Net Radiation, Soil Heat Flux and Sensible Heat Flux, respectively. All ET data from OpenET are at a spatial resolution of Landsat satellite data of 30 × 30 m.

2.6 | Statistics

We used a mixed effects linear regression model to evaluate the influence of air temperature, relative humidity and vapour pressure deficit (VPD) on leaf water potential, Ψ_{leaf}. Air temperature, relative humidity and VPD were treated as fixed effects and tree ID was treated as the random effect using the 'lme4' package (Bates et al. 2015) in R (R Core Team 2019). We also used an ANOVA with a post hoc Tukey HSD test to examine differences in Ψ_{leaf} among sites (OG and DT TT) for individual dates across the monsoon season. Finally, we used an ANOVA with a post hoc Tukey HSD test to determine significant difference among plot level mean $\delta^{18}O_{xylem}$ (OG, DT TT and UL) at different times of the year to examine differences in source water use among treatments.

3 | Results

3.1 | Site Climate

The precipitation patterns at Three Links generally showed a bimodal precipitation regime. Three Links received 388 mm of precipitation during the 2022 water year (1 October 2021–30 September 2022); of the total, only 33 mm fell during the winter from December to February, 317 mm fell during the monsoon season between June and September, and the remaining 39 mm fell during other times of the year (Figure 2). Regionally, this was the ninth wettest monsoon on record over a 127-year monitoring period (NOAA 2023). During the 2023 water year, 227 mm of total precipitation fell, with 87 mm falling during the winter, 90 mm falling during the monsoon season and 50 mm falling during the other times of the year. The drier winter/wetter monsoon season in 2022 compared to the wetter winter/drier monsoon season of 2023 provided an opportunity to examine how differences in bimodal precipitation influence tree water use.

The 11-year annual precipitation average in nearby Cascabel, AZ was 342 ± 75.49 mm (Arizona State Climate Office 2022).

Despite 2022 being a wetter year overall, it had more extreme temperatures and a higher maximum VPD than 2023. During the 2022 water year, the maximum daily temperature reached 46.2°C and the minimum reached −13.5°C (Figure 2). During the same period, the maximum daily average VPD reached 4.2 kPa (Figure 2). During the 2023 water year, the maximum daily temperature reached 44.2°C and the minimum −11.2°C (Figure 2). Maximum daily average VPD reached 3.9 kPa (Figure 2).

In the 2022 water year, on average, soil VWC from the DT plots tended to be higher (0.20 ± 0.01 m^3/m^3 at 30 cm), followed by the TT (0.13 ± 0.03 m^3/m^3 at 30 cm) and the OG (0.13 ± 0.01 m^3/m^3 at 30 cm). Across the season, VWC was highest following the monsoon rains; in the OG and TT plots, this occurred during late August (OG: 0.179 m^3/m^3; TT: 0.289 m^3/m^3) and in mid-September for the DT plot (0.227 m^3/m^3). The lower VWC occurred during the winter in January for the OG and TT (OG: 0.116 m^3/m^3; TT: 0.118 m^3/m^3) and early February for the DT (0.18 m^3/m^3) (Figure 3). In the 2023 water year, on average, soil VWC from the DT plots tended to be higher (0.24 ± 0.03 m^3/m^3

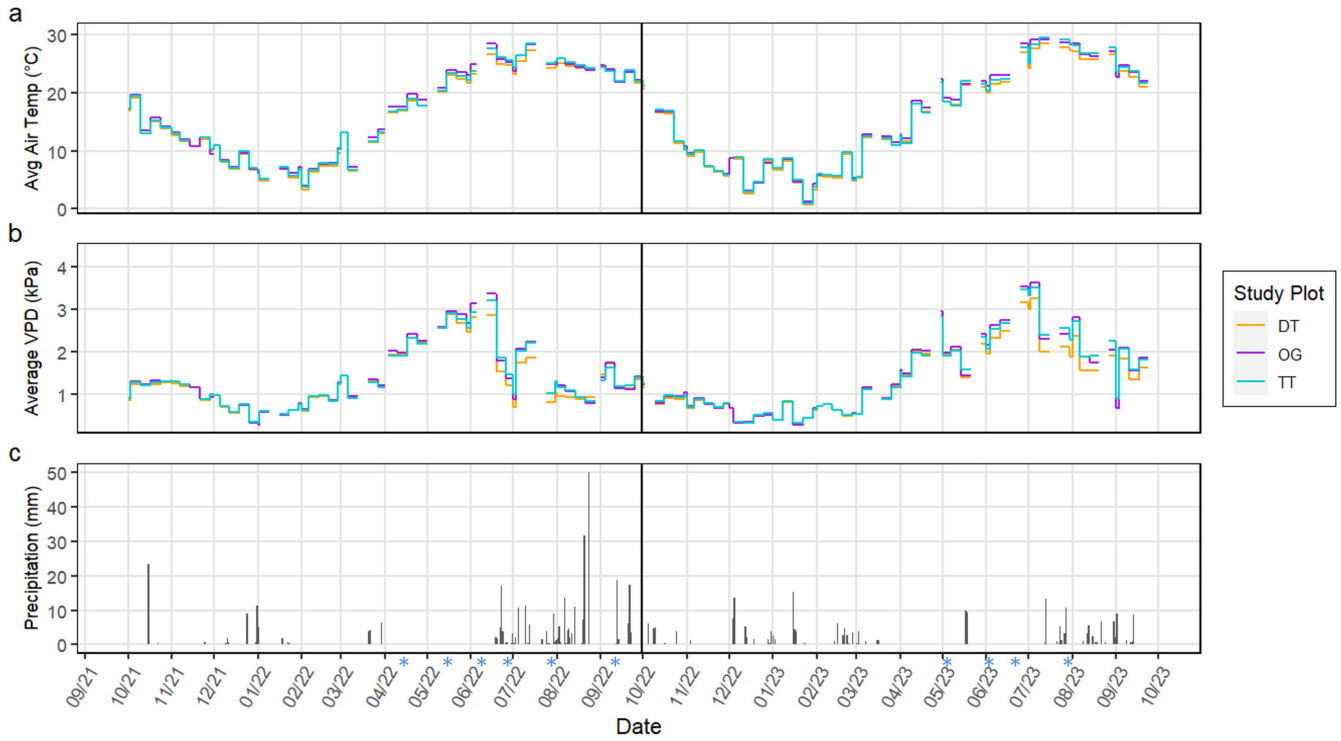

FIGURE 2 | (a) Weekly average air temperature (°C), (b) weekly average vapour pressure deficit (VPD; kPa) and (c) daily total precipitation (mm) for the three plots, old growth (OG), dense thicket (DT) and thinned thicket (TT). The black line separates the 2022 and 2023 water years. Asterisks indicate dates of leaf water potential collection.

FIGURE 3 | Soil volumetric water content (m^3/m^3) measured at two depths, 10 cm and 30 cm, for the three study plots: old growth, dense thicket and thinned thicket. The black line separates the 2022 and 2023 water years.

at 30 cm), followed by the TT ($0.17 \pm 0.03\ m^3/m^3$ at 30 cm) and the OG ($0.14 \pm 0.01\ m^3/m^3$ at 30 cm). When comparing between the 2 years, winter precipitation in 2023 led to higher soil VWC at 30 cm than in 2022 (Figure 3). For summer precipitation, the more abundant and frequent monsoon rains in 2022 led to more frequent wetting of the near surface soil while the weaker 2023 monsoon had a very muted impact on soil moisture.

3.2 | Leaf Area Index

Using on-site observations, we noted that the mesquite in the OG, DT and TT plots began to leaf out in late April of 2022 while those of the UL leafed out in early April. Using LAI measurements, we found the DT and TT canopy density increased rapidly from May to June (0.62 to $1.77\ m^2/m^2$ and 0.28 to $0.69\ m^2/m^2$, respectively), while the OG plot leafed out more slowly (1.04 to 1.1). Canopy density continued to increase through mid-July in the DT and OG plots (1.77 to 2.17 and 1.1 to 1.41, respectively), while it remained constant in the TT (0.69 to 0.68) (Figure 1).

3.3 | Evapotranspiration

We totaled the monthly ET data from the 2019–2023 water years and found that the DT and OG were very similar (Table 1). ET was much higher than mean annual or yearly precipitation (~350 mm) at the TT, DT and OG sites, while it was closest to precipitation values at the UL. TT averaged 99.1 cm across the 5-year period and was consistently lower than DT (avg of 108.2 cm) and OG (avg of 109.5 cm). The UL (avg of 42.5 cm) stand was consistently lowest of all, and it declined in the low-rainfall year (2023), while the other sites increased slightly. After the thinning treatment was administered in February of 2022, the yearly total ET at the TT plot decreased from 104.3 cm in 2021 to 83.2 cm in 2022 followed by 90.8 cm in 2023.

3.4 | Oxygen and Hydrogen Isotopes

By using local precipitation hydrogen (δ^2H) and oxygen ($\delta^{18}O$) isotope values, we created a local meteoric water line; as expected, summer monsoon precipitation was more $\delta^{18}O$ enriched (-4.9 ± 2.2‰ $\delta^{18}O$ and -34 ± 16‰ δ^2H) than winter precipitation (-7.2 ± 2.2‰ $\delta^{18}O$ and -47 ± 20‰ δ^2H). Deep groundwater was even more depleted (-9.0 ± 0.4‰ $\delta^{18}O$ and -65 ± 2‰ δ^2H) than winter precipitation (Figure 4), which supports previous studies that found groundwater in this area to be recharged from winter precipitation infiltrating along distant mountain fronts (Eastoe and Towne 2018). We found the summer LMWL to have a slope of 6.69, while the winter LMWL had a slope of 7.59. In our figures and analysis, we use a total year LMWL with a slope of 6.82.

During the 2022 and 2023 water years, the shallower soils (5 cm) were slightly more isotopically enriched in $\delta^{18}O$ (−9.8‰ to 11.8‰) than the deeper soils (50 cm) (−11.0‰ to −0.7‰), which is consistent with the process of evaporative enrichment (Figure 4). In 2022, the difference between the upper 5 cm and deeper 50 cm increased during May 6 and June 9 for all four plots (Figure 4); this coincided with when VPD was increasing (Figure 2) and shallow soils were becoming more dry (Figure 3). After the arrival of the summer monsoon rains in mid-June, the difference between the upper 5 cm and deeper 50 cm decreased for the collection dates of June 27 and August 28, though not for July 19. In 2023, the difference between the upper 5 cm and deeper 50 cm for all four plots increased between May 25 and June 23 (Figure 4); this also coincided with when VPD was increasing (Figure 2) and shallow soils were becoming more dry (Figure 3). The exception was in May, when recent precipitation led to similar values in $\delta^{18}O_{soil}$ between the upper and deeper soils. After the arrival of the summer monsoon rains in mid-July, the difference between the upper 5 cm and deeper 50 cm decreased on July 16 but then increased again by August 20. We did not observe any consistent differences in the $\delta^{18}O_{soil}$ profile among the four sites, although deeper soils (50 cm) from the OG sites tended to be more negative (Figure 4).

In 2022, while $\delta^{18}O_{xylem}$ varied throughout the year and across sites, there were some general patterns. First, in all the sites, we found that during spring (May 6), $\delta^{18}O_{xylem}$ was highly enriched (Figure 5 and Figure 6). Since the trees were dormant and not taking up new water, the $\delta^{18}O_{xylem}$ likely reflected increasing enrichment due to evaporation of stem water taken up during the previous fall. We included these values to clearly show the change between the period before leafing out and after. Second, as the trees began to leaf out and prior to the arrival of monsoon rains, $\delta^{18}O_{xylem}$ values during June 9 were all negative and highly clustered along the LMWL (average of $-5.5‰ \pm 1.6‰$), indicating that trees were using deeper soil water that had not experienced evaporative enrichment. Third, with the arrival of the summer monsoon rains, $\delta^{18}O_{xylem}$ values became more enriched and fell to the right of the LMWL; this indicates that trees were likely using shallow soil water that had a monsoon rain isotopic signature, which had also undergone some evaporative enrichment in the heavy isotope. This pattern is also evident in Figure 6, in which the xylem water isotopes overlap with the shallow soil and precipitation isotopes during and shortly after the monsoon season, especially in 2022. We note that during the September 2022 collection date, the 5-cm soil water value overlapped with the groundwater $\delta^{18}O$ values; this could be due to a recent precipitation event with similarly negative $\delta^{18}O$ values to that of groundwater, which did not penetrate to the lower soil depths (Figure 6).

We found site level differences in $\delta^{18}O_{xylem}$ during some sampling dates, although these differences were not consistent across the growing seasons. At the start of the growing season, the trees at the UL plot began to leaf out the earliest in late April/early

TABLE 1 | Estimated total annual evapotranspiration at each study plot as determined by the geeSEBAL v0.2.2 model.

Year	TT	DT	OG	UL
2019	40.15748	42.6378	42.12598	16.92913
2020	45.27559	48.4252	48.46457	17.24409
2021	41.06299	42.83465	43.18898	17.00787
2022	32.75591	38.77953	40.74803	17.3622
2023	35.74803	40.35433	41.06299	15.03937

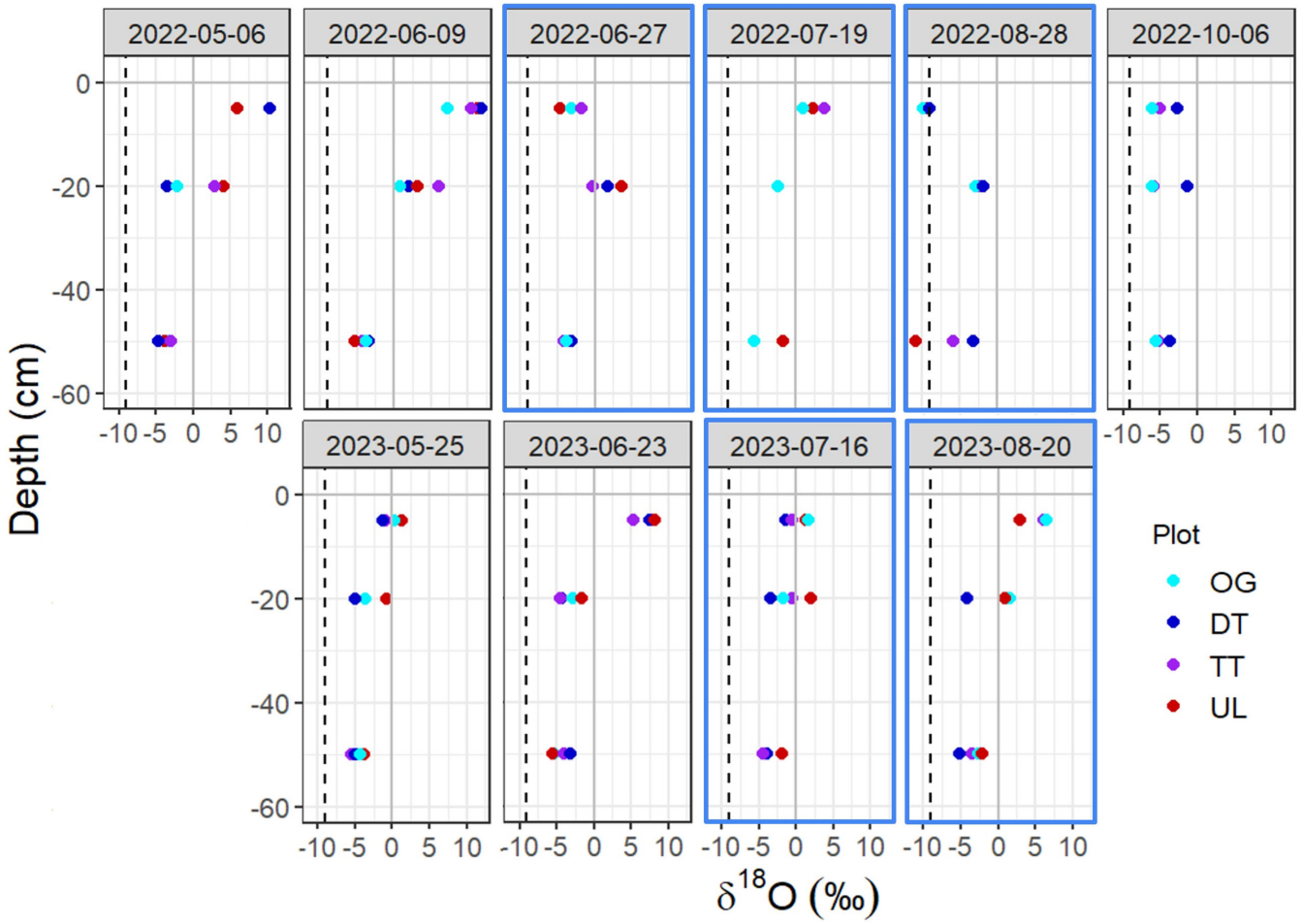

FIGURE 4 | Oxygen ($\delta^{18}O$) isotopes of shallow soil layers for the four study plots: old growth (OG), dense thicket (DT), thinned thicket (TT) and upland (UL). Plots bordered in blue indicate sample dates during the monsoon rain season. Vertical dotted black line indicates average $\delta^{18}O$ of groundwater.

May and began taking in new water as indicated by $\delta^{18}O_{xylem}$ values that clustered close to the LMWL (−6.0‰ ± 1.5‰) on May 6. This contrasts with the DT and TT sites that had more enriched average $\delta^{18}O_{xylem}$ values of 4.2‰ ± 5.0‰ and 1.4‰ ± 5.5‰ ($p = 0.0003$ and $p = 0.006$, respectively); we also found that DT values were statistically different from OG (−2.7‰ ± 3.9‰) ($p = 0.02$). Since the DT, TT and OG trees had not leafed out yet by May 6 (trees in these plots began leafing out in late May), the enriched $\delta^{18}O_{xylem}$ water suggests these trees were not actively taking up soil water. During the monsoon season on July 19, $\delta^{18}O_{xylem}$ was the most enriched at the TT site (−6.3‰ ± 0.6‰) followed by the DT site (−6.2‰ ± 0.2‰), the OG site (−5.5‰ ± 1.8‰) and the UL site (−3.7‰ ± 0.9‰). At another period during the growing season on August 28, DT $\delta^{18}O$ was more enriched (−3.8‰ ± 1.3‰) than OG (−6.2‰ ± 0.6‰) ($p = 0.02$) and UL (−7.1‰ ± 1.0‰) ($p = 0.003$). We did not find a statistical difference between DT and TT (−4.9‰ ± 2.7‰). By December, trees at all plots had dropped their leaves and their increasingly $\delta^{18}O$ enriched water (2.5 ± 3.5‰ DT, 3.8 ± 4.4‰ OG, 4.8 ± 6.6‰ UL and 5.7 ± 4.5‰ TT) indicated no recent water uptake (Figures 5, S1, S2, S3 and S4).

In 2023, there were no statistically significant $\delta^{18}O_{xylem}$ differences between the plots on any of the sampling dates. Trees across all plots leafed out on a similar time frame to one another and were nearly fully leafed out by May 25 when all the plots had isotope ratio values of xylem water clustered near the LMWL with a mean $\delta^{18}O_{xylem}$ of −2.3‰ ± 4.3‰. Just prior to the first monsoon rains on June 23 to after the monsoon rains on August 20, there was little to no change in the average $\delta^{18}O_{xylem}$ (June 23 $\delta^{18}O_{xylem}$: −3.2‰ ± 3.9‰; July 16 $\delta^{18}O_{xylem}$: −2.0‰ ± 4.2‰; August 20 $\delta^{18}O_{xylem}$: −2.6‰ ± 5.5‰). On each of these dates, the $\delta^{18}O_{xylem}$ values fell to the right of the meteoric water line, indicating that the trees were using highly $\delta^{18}O$ enriched water (most likely shallow soil water) (Figures 5 and 6).

3.5 | Leaf Water Potential

In 2022, average predawn leaf water potential (Ψ_{PD}) of all three riparian sites declined from the beginning of the summer (May 6) until August 18, even after the arrival of summer precipitation. By October 6, Ψ_{PD} for the OG site continued to decline to its lowest level of the summer (−2.26 ± 0.36 MPa), while that at both the DT (−1.41 ± 0.16 MPa) and the TT sites (−1.4 ± 0.26 MPa) increased (Figure 7). Both Ψ_{PD} of DT and TT were statistically different from the OG in October ($p < 0.0001$ and $p < 0.0001$). Average midday leaf water potential (Ψ_{MD}) of all three sites

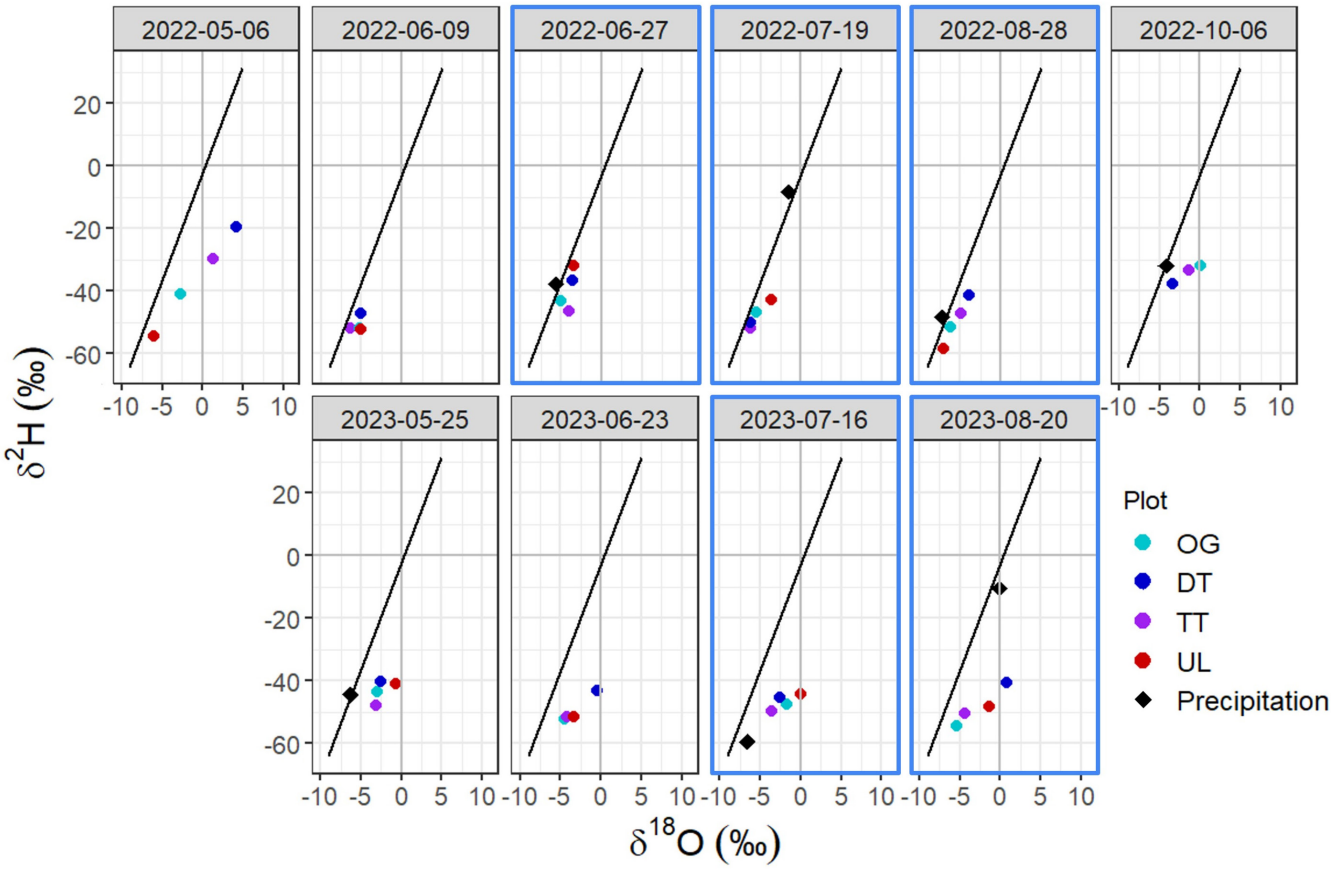

FIGURE 5 | Averaged oxygen ($\delta^{18}O$) and hydrogen ($\delta^{2}H$) isotopes from tree xylem for the four study plots: old growth (OG), dense thicket (DT), thinned thicket (TT) and upland (UL). Plots bordered in blue indicate sample dates during the monsoon rain season. Precipitation is also plotted on the local meteoric water line.

also declined from the beginning of the summer (May 6) until the end of the monsoon season (October 6). In May of 2022, TT exhibited the least negative Ψ_{MD} (−1.51 ± 0.19 MPa) followed by DT (−1.79 ± 0.17 MPa), with OG showing the most negative Ψ_{MD} (−2.3 ± 0.26 MPa) (OG-DT: $p < 0.0001$; OG-TT: $p < 0.0001$; TT-DT: $p = 0.04$). By mid-August, Ψ_{MD} was more negative for all plots and continued to decline into early October at OG (−3.44 ± 0.41 MPa), while both TT (−2.26 ± 0.43 MPa) and DT (−1.94 ± 0.57 MPa) increased (Figures 7, S5, S6 and S7). OG was significantly different from DT ($p < 0.0001$) and TT ($p < 0.0001$).

In 2023, average Ψ_{PD} of the three plots showed little change from May until late August. By the middle of August, which was the last date sampled in 2023, Ψ_{PD} was least negative for TT (−1.36 ± 0.14 MPa) and significantly different from DT (−1.72 ± 0.22 MPa; $p = 0.003$) and OG (−1.73 ± 0.24 MPa; $p = 0.002$) (Figure 7). Average Ψ_{MD} declined across all plots from May until late August. In May of 2023, DT had the least negative Ψ_{MD} (−1.72 ± 0.31 MPa) and was significantly different from TT (−2.2 ± 0.42 MPa; $p = 0.03$) and the OG (−2.26 ± 0.37 MPa; $p = 0.01$). By the middle of August, the last date sampled in 2023, Ψ_{MD} was the most negative for the entire season, with TT as the least negative (−2.81 ± 0.28 MPa) and significantly different from DT (−3.18 ± 0.35 MPa; $p = 0.05$) and OG (−3.47 ± 0.29 MPa; $p = 0.001$) (Figures 7, S5, S6 and S7). We also examined the impact of tree size on both Ψ_{PD} and Ψ_{MD} and found no significant differences among size classes.

To evaluate the importance of different environmental factors in determining Ψ_{MD}, we used multiple linear regression models to evaluate air temperature, relative humidity, vapour pressure deficit and Ψ_{soil} at each of the test plots. We found that only relative humidity was significant at the OG site ($p = 0.02$), while air temperature, relative humidity and vapour pressure deficit were significant at the DT (air temp: $p = 0.0000$, relative humidity: $p = 0.0004$, VPD: $p = 0.0000$) and air temperature, relative humidity, vapour pressure deficit and Ψ_{soil} were significant at the TT site (air temp: $p = 0.0000$, relative humidity: $p = 0.003$, VPD: $p = 0.0000$, Ψ_{soil}: $p = 0.0000$)(Figure 2).

4 | Discussion

In this study, we leveraged a unique opportunity to examine the water-use strategies of riparian mesquite stands differing in both age structure and density. The thicketization of an abandoned agricultural field in this riparian area can be viewed as a natural progression of succession. Contary to expectation, our findings revealed that, across two water years, the different stands of mesquite exhibited similar patterns in their source water use, relying on both shallow and deep soil moisture despite differences in tree age, size and density of the stands. Mesquite started using deep soil water and/or groundwater as soon as they leafed out in the early summer and then incorporated shallow soil moisture from the discrete monsoon rains pulses when

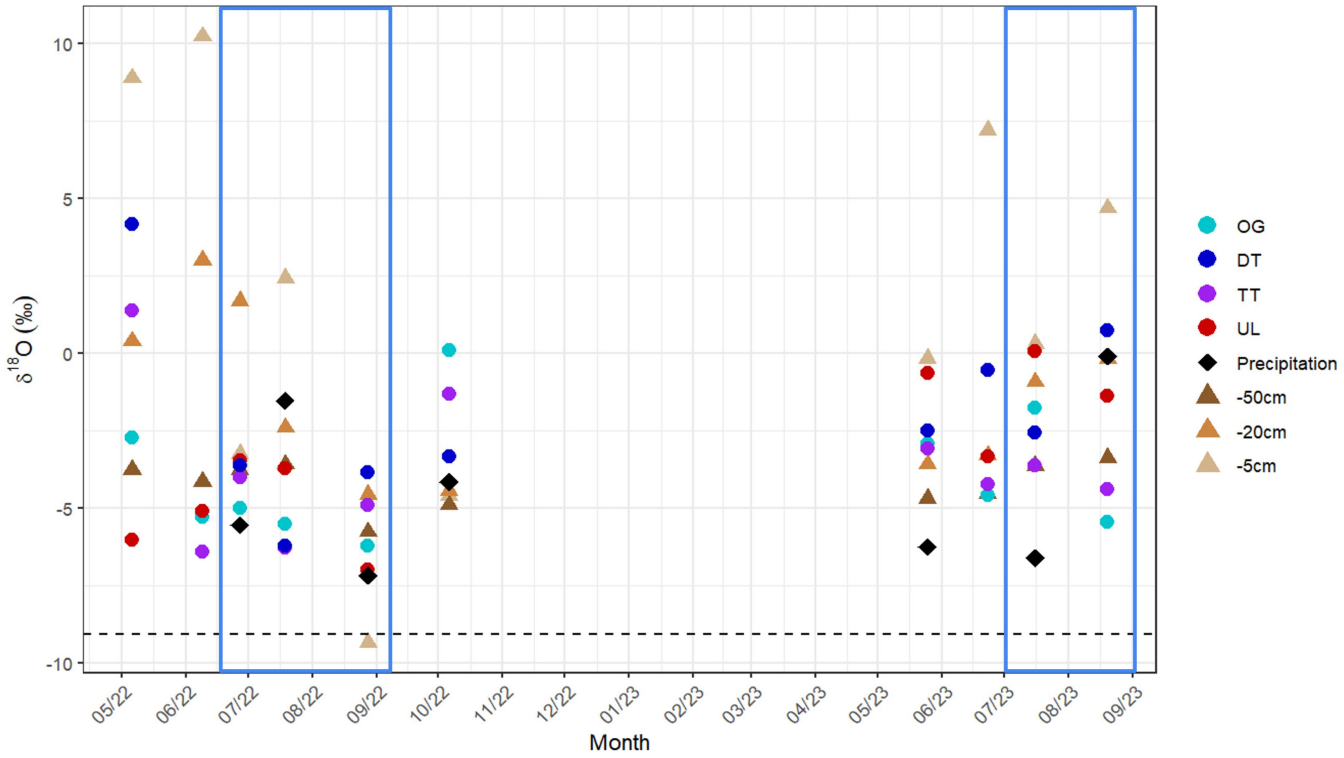

FIGURE 6 | Combined $\delta^{18}O$ values for plant xylem (circles), soil (triangles) and precipitation (diamonds). Blue boxes indicate months with monsoon rainfall. Horizontal dotted black line indicates average $\delta^{18}O$ of groundwater.

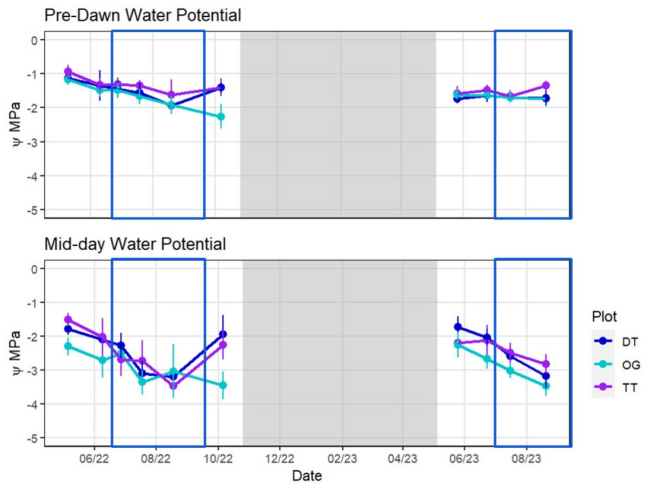

FIGURE 7 | Ψ_{leaf} (leaf water potential) during summer of 2022 and 2023 for the four study plots: old growth (OG), dense thicket (DT) and thinned thicket (TT). Blue boxes indicate months with monsoon rainfall.

it became available. We also found that despite decreasing Ψ_{MD} throughout the monsoon season, most mesquite close to the riparian corridor (TT, DT and OG) did not exceed the critical Ψ_{MD} values (Figure 7) typically observed in water stressed mesquites (Hultine et al. 2006; Pockman and Sperry 2000)—by which we mean those experiencing severe cavitation. Interestingly, Ψ_{MD} continued to decrease over the course of the growing season, despite the addition of monsoon rains and lower atmospheric VPD, which we expected would yield less negative Ψ_{MD}. Also of interest, Ψ_{PD} in all sites decreased more throughout the monsoon season in 2022 than in 2023, even though the monsoon season of 2022 had 111% (317 vs. 90 mm) more precipitation at the study site than in 2023. However, while the monsoon season of 2023 was underwhelming, there was 91% (33 vs. 87 mm) more winter precipitation in 2023 than in 2022 in the study site; we posit that higher winter precipitation in 2023 led to deeper soil moisture recharge which played an important role in helping trees maintain a relatively high Ψ_{PD} throughout the entire growing season, despite experiencing less summer precipitation.

4.1 | Similar Source Water Across Plots

Though mesquite source water shifted across the growing season showing the species' flexibility in water use as a facultative phreatophyte, it did not vary substantially between test plots, and younger trees (DT and TT) did not use different sources of water than mature trees (OG) except for slight differences in timing. Our findings suggest that mature and young mesquite trees used similar sources of water along the soil profile in the riparian area, while mesquite trees growing in the upland area began using soil water slightly earlier than those in the riparian plots, likely because they leafed out earlier (Figure 6). The similar source water for young and mature trees is likely explained by both the tendency of young trees to devote substantial energy into root growth in their early stages (Stromberg 1993; Zimmermann 1969) as well as the relatively shallow water table in this area. In June 2022 after trees had leafed out, xylem water isotope values plotted near the LMWL indicated a reliance on deeper soil water and/or groundwater since there had not been any recent precipitation (Scott, Huxman, et al. 2006). Once the monsoon began, we found shallow soil water became

an additional source (Scott, Huxman, et al. 2006; Snyder and Williams 2000). The depth to groundwater at our sites normally did not exceed 10 m, which is within the reported rooting depth for mesquite (Stromberg et al. 1992; Zimmermann 1969) and well in range for the trees to reach the capillary fringe that they are known to draw from (Scott, Huxman, et al. 2006; Stromberg et al. 1992; Stromberg 1993; Snyder and Williams 2000).

Differences in xylem water values between the 2023 water year and the 2022 water year may be explained by a wetter winter, a wetter May and a drier monsoon in 2023. Xylem isotope values from late May 2023 plotted near the precipitation isotope value taken from the mid-May rain event (Figure 6) indicated that shallow roots remained active and were able to use that resulting shallow soil moisture (Figure 3). While it is unclear if the wetter winter helped keep shallow roots active when they otherwise might not be, it is possible that the wetter winter allowed trees to leaf out earlier and faster than in 2022, leaving them better poised to take advantage of the mid-May precipitation (Glendening and Paulsen 1955; Nilsen et al. 1991; Scott, Goodrich, et al. 2006; Armstrong-Herniman and Greenwood 2021). Later, in the summer of 2023, the trees used more shallow soil moisture, which had undergone more evaporative enrichment in the heavy isotope due to the drier monsoon season, as indicated by the more enriched $\delta^{18}O_{xylem}$ values measured in July and August of 2023 compared to 2022.

The slight differences in the $\delta^{18}O_{xylem}$ of the UL plot from the other plots, specifically in May of 2022, were likely due to these trees leafing out earlier and taking up new water before the trees of the other plots became active. The other trees continued to have more enriched $\delta^{18}O_{xylem}$ values in May because their stem water was likely undergoing evaporative enrichment during the period before leaf expansion (June 2021). While Hultine et al. (2004) found that hydraulic redistribution can continue to occur throughout the root system even during periods of crown dormancy, our study was not designed to measure this. Another explanation for the slight differences in the UL plot could be attributed to its trees having more limited access to groundwater than other stands. Although xylem water isotope trends suggest the UL had similar access to source water to the other stands, it is important to note that isotope analysis cannot easily distinguish between water from the deep unsaturated zone and the deeper saturated zone/capillary fringe, both being regions where evaporative enrichment of $\delta^{18}O$ does not occur (Barnes and Turner 1998; Wu et al. 2023). Also, the diminutive tree size at the UL plot suggests the mesquite do not have a sufficient water supply required for them to reach the stand density and tree stature of the mature stands along riparian areas (Stromberg 1993). It has been established that the larger tree form of mesquite bosques requires groundwater depths <15 m, so the greater groundwater depth at the UL plot implies they may be unable to tap into the groundwater at the capillary fringe (Brown 1982; Stromberg et al. 1992; Stromberg 1993).

There were some outlying values in July and August of 2023 with excessively enriched $\delta^{18}O$. We considered that these enriched values could be explained as the trees drawing from tightly bound soil water held since the previous rainy season, as suggested by Renée Brooks et al. (2009). We determined this explanation was unlikely as that process would require soil moisture to be at its seasonal lowest in order for the trees to resort to drawing on that tightly bound soil water; however, the months during which the excessively $\delta^{18}O$ enriched values occurred (July–August 2023) did not experience excessively dry soils (OG: 13.4%; DT: 24.6%; TT: 14.2%) VWC compared to 2022 (OG: 13.6%; DT: 21.4%; TT: 16.9% soil moisture) (Figure 3). It is more likely that in 2023, the trees were using monsoon precipitation, which had undergone more evaporative $\delta^{18}O$ enrichment (because of less frequent and smaller precipitation events) compared to 2022, when the trees were using monsoon precipitation that had undergone less evaporative $\delta^{18}O$ enrichment because of more frequent and larger precipitation events.

4.2 | Decreasing Water Potential After Monsoon Onset

Throughout the premonsoon and monsoon seasons, there was a trend across all riparian plots of gradually decreasing Ψ_{MD}. Our 2022 data revealed that water stress in mesquite was not alleviated with the onset of monsoon rains but instead increased only towards the conclusion of the monsoon season, specifically after August. In 2023, there was no apparent response in Ψ_{leaf} to the monsoon even though the monsoon period was drier compared to 2022. Surprisingly, despite the drier monsoon season of 2023, Ψ_{MD} reached the same low value of -3.47 MPa in both years (Figures 2 and 7). The fact that Ψ_{leaf} during a drier monsoon year led to the same Ψ_{leaf} as a wet monsoon year suggests that a wetter winter season in 2023 may have buffered the trees against the dry summer (Brown et al. 1997; Schenk and Jackson 2002). Because winter precipitation tends to infiltrate more deeply and less evaporative loss occurs during winter compared to summer, more winter precipitation allows deeply rooted woody plants to have greater access to deeper soil moisture (Brown et al. 1997; Reynolds et al. 2004; Schenk and Jackson 2002). This phenomenon was observed by Brown et al. (1997) for a multidecadal period of greater winter precipitation. Hultine et al. (2004) also found that a significant amount of water is redistributed downward by mesquite during winter dormancy when shallow soils are wetted, allowing trees to 'bank' water for later use. It has also been established that in the San Pedro basin, winter precipitation along mountain fronts and summer precipitation from summer flood flows contribute approximately equally to groundwater recharge (Eastoe and Towne 2018), so in years with less summer precipitation, winter precipitation is likely even more important.

The decline of Ψ_{MD} even across the monsoon may be attributed to an anisohydric strategy that prioritizes carbon assimilation over water loss regulation (stomatal conductance remains higher, Ψ_{MD} continues to decrease). This strategy is known to occur in *Prosopis glandulosa*, a closely related species, as well as *Larrea tridentata*, both of which are common in the Southwest (Guo et al. 2020; Nilsen et al. 1981). The decline in Ψ_{leaf} was particularly notable in the OG plot where Ψ_{PD} and Ψ_{MD} levels were usually more negative than the other plots and reached as low as -3.47 ± 0.29 MPa. These mature, larger trees may have different strategies of stomatal regulation due to more consistent groundwater access compared to trees in younger stands (Giordano et al. 2011).

As midday water potential declined through the season, average Ψ_{MD} for one plot did reach a low of −3.47 MPa, which is lower than water potentials at which 50% loss of hydraulic conductivity in stems (P50) has been reported in previous studies (−2.56 MPa; Hultine et al. 2019). However, studies have found that in some angiosperms, the point of no return is closer to 88% (P88) (Meinzer and McCulloh 2013). Stomatal closure in *P. glandulosa*, a closely related species, is triggered only when Ψ_{leaf} levels drop below −4.0 MPa (Nilsen et al. 1983). Hultine et al. (2006) suggest that upland mesquite in sandy loam soils undergo 95% loss of conductance at −11.57 MPa, while Pockman and Sperry (2000) found 100% embolism at −5.0 MPa for riparian mesquite. This suggests that the observed Ψ_{MD} levels for mesquite in our plots remained well within a tolerable range.

Through multiple linear regression modelling, we found differences in the significance of air temperature, relative humidity and VPD for determining Ψ_{leaf} across the plots. Because air temperature, relative humidity and VPD were significantly different at the DT site, but not the OG site, this suggests that something other than these environmental factors may be responsible at the OG site. A likely possibility could be differences in soil composition, which directly impacts soil hydraulic properties and thus, plant water availability (Hultine et al. 2006). While we did not classify soil type or analyse grain size, we did observe that the OG site had sandier soils, while the DT and TT had more clay-rich soils, which may impact the Ψ_{leaf} much more than the slight variations in climatic factors between plots. This is because, in coarse-textured soils like that of the OG, the higher unsaturated hydraulic conductivity leads to higher infiltration rates but lower soil water content (Hultine et al. 2006) (Figure 3). As a result, Ψ_{leaf} in OG may have been more negative than expected (given that older mesquite trees likely have a more extended root system for water acquisition) because of the sandier soil in which they grew.

4.3 | Evapotranspiration

All stands at Three Links except the UL plot appear to access and use some groundwater because ET exceeds precipitation (by ~100%); The UL plot has estimated ET values much closer to precipitation values. The UL plot was also more affected by the low-rainfall year. The $\delta^{18}O_{xylem}$ data also suggest that while the trees in the riparian area were not simply using groundwater, they were likely using a mixture of groundwater and unsaturated soil water (Figure 4). This indicates much reduced use of groundwater and/or deep soil moisture by the UL trees and is reflected by their much smaller sizes and density compared to the plots closer to the river (Bodner 2025). The thinning treatment applied to the TT in 2022 decreased the amount of ET measured compared to pretreatment years. This effect is consistent with results seen in other studies of different tree species in different forest types (Chiu et al. 2022; Isaacson et al. 2023). The diminished impact on ET over time of the TT plot by 2023 has also been previously documented (Isaacson et al. 2023). It is likely that the impact of thinning on ET would continue to diminish in subsequent years due to increased light penetration driving higher soil water evaporation as well as greater transpiration from the herbaceous cover in the understory (Simonin et al. 2007). Interestingly, despite the decrease in ET in the TT plots, we did not find any significant differences in water-use strategies or Ψ_{leaf} between the TT and DT plots.

5 | Conclusion

Because mesquite occurs across many dryland regions and shares functional traits with other facultative phreatophytes, the patterns we observed may reflect broader water-use behaviours common in arid and semi-arid ecosystems. Our findings therefore contribute to a tentative framework for understanding how woody plants balance deep and shallow water sources under variable seasonal precipitation. While this study found that mesquite relied primarily on shallow groundwater and/or deep soil moisture during dry months and also took advantage of shallow soil moisture from precipitation when available, it was beyond the scope of this study to speculate on the degree of impact this could have on groundwater levels and thus on streamflow. Furthermore, it is presently unclear how water-use strategies may be impacted by further groundwater decline. Presumably, if groundwater levels remain the same or increase then there may be ample opportunity for mesquite bosque restoration in this area, as demonstrated at this study site. However, if groundwater levels decline or do so abruptly, how such declines might impede restoration efforts or how degradation of mesquite bosques might alter their form and function warrants future investigation.

Acknowledgements

This research was supported by the Nature Conservancy, USDA-ARS and the University of Arizona. We would like to thank the many people who provided help with field data collections and general assistance throughout the project, including (but not limited to) Kathleen Kleinschmidt, Jessie Pearl, Bob Rogers, Kinzie Bailey, Taylor McCoy, Ceci Martinez, David Kierys and other employees of the Nature Conservancy.

Data Availability Statement

The data that support the findings of this study are available from the corresponding author upon reasonable request.

References

Adams, D. K., and A. C. Comrie. 1997. "The North American Monsoon." *Bulletin of the American Meteorological Society* 78, no. 10: 2197–2213. https://doi.org/10.1175/1520-0477(1997)078<2197:tnam>2.0.co;2.

Allen, S. T., J. W. Kirchner, S. Braun, R. T. W. Siegwolf, and G. R. Goldsmith. 2019. "Seasonal Origins of Soil Water Used by Trees." *Hydrology and Earth System Sciences* 23, no. 2: 1199–1210. https://doi.org/10.5194/hess-23-1199-2019.

Archer, S., C. Scifres, C. R. Bassham, and R. Maggio. 1988. "Autogenic Succession in a Subtropical Savanna: Conversion of Grassland to Thorn Woodland." *Ecological Monographs* 58, no. 2: 111–127. https://doi.org/10.2307/1942463.

Archer, S. R., and K. I. Predick. 2014. "An Ecosystem Services Perspective on Brush Management: Research Priorities for Competing Land-Use Objectives." *Journal of Ecology* 102, no. 6: 1394–1407. https://doi.org/10.1111/1365-2745.12314.

Archer, S. R., E. M. Andersen, K. I. Predick, S. Schwinning, R. J. Steidl, and S. R. Woods. 2017. *Woody Plant Encroachment: Causes and*

Consequences, 25–84. Springer Series on Environmental Management. https://doi.org/10.1007/978-3-319-46709-2_2.

Arizona State Climate Office. 2022. COOP Sites Arizona. "IEM:: Monthly Summaries." Iowa Environmental Mesonet, 2022, mesonet.agron.iastate.edu/sites/monthlysum.php?network=AZ_DCP&station=ZBKA3.

Armstrong-Herniman, W., and S. Greenwood. 2021. "The Role of Winter Precipitation as a Climatic Driver of the Spring Phenology of Five California *Quercus* Species (Fagaceae)." *Madroño* 68, no. 4: 450–460. https://doi.org/10.3120/0024-9637-68.4.450.

Barnes, C. J., and J. V. Turner. 1998. "Chapter 5—Isotopic Exchange in Soil Water." In *Isotope Tracers in Catchment Hydrology*, edited by C. Kendall and J. J. McDonnell, 137–163. Elsevier. https://doi.org/10.1016/B978-0-444-81546-0.50012-4.

Bastiaanssen, W. G. M., M. Menenti, R. A. Feddes, and A. A. M. Holtslag. 1998. "A Remote Sensing Surface Energy Balance Algorithm for Land (SEBAL). 1. Formulation." *Journal of Hydrology* 212: 198–212. https://doi.org/10.1016/s0022-1694(98)00253-4.

Bastiaanssen, W. G. M., H. Pelgrum, J. Wang, et al. 1998. "A Remote Sensing Surface Energy Balance Algorithm for Land (SEBAL)." *Journal of Hydrology* 212–213: 213–229. https://doi.org/10.1016/s0022-1694(98)00254-6.

Bates, D., M. Mächler, B. Bolker, and S. Walker. 2015. "Fitting Linear Mixed-Effects Models Using lme4." *Journal of Statistical Software* 67, no. 1: 1–48. https://doi.org/10.18637/jss.v067.i01.

Bodner, G. S. 2025. *Becoming Bosque: Testing the Benefits of Mesquite Restoration*. Nature Conservancy.

Brown, D. E. 1982. *Biotic Communities of the American Southwest—United States and Mexico*. Desert Plants.

Brown, J. H., T. J. Valone, and C. G. Curtin. 1997. "Reorganization of an arid ecosystem in response to recent climate change." *Proceedings of the National Academy of Sciences* 94, no. 18: 9729–9733. https://doi.org/10.1073/pnas.94.18.9729.

Brunel, J.-P., G. R. Walker, and A. K. Kennett-Smith. 1995. "Field Validation of Isotopic Procedures for Determining Sources of Water Used by Plants in a Semi-Arid Environment." *Journal of Hydrology* 167, no. 1–4: 351–368. https://doi.org/10.1016/0022-1694(94)02575-v.

Castagneri, D., G. Vacchiano, A. Hacket-Pain, R. J. DeRose, T. Klein, and A. Bottero. 2022. "Meta-Analysis Reveals Different Competition Effects on Tree Growth Resistance and Resilience to Drought." *Ecosystems* 25, no. 1: 30–43. https://doi.org/10.1007/s10021-021-00638-4.

Chen, Y., B. R. Helliker, X. Tang, F. Li, Y. Zhou, and X. Song. 2020. "Stem Water Cryogenic Extraction Biases Estimation in Deuterium Isotope Composition of Plant Source Water." *Proceedings of the National Academy of Sciences* 117, no. 52: 33345–33350. https://doi.org/10.1073/pnas.2014422117.

Chiu, C.-W., T. Gomi, M. Hiraoka, K. Shiraki, Y. Onda, and B. X. Dung. 2022. "Evaluating Changes in Catchment-Scale Evapotranspiration After 50% Strip-Thinning in a Headwater Catchment." *Hydrological Processes* 36, no. 6: e14611. https://doi.org/10.1002/hyp.14611.

Conway, B. D. 2016. "Land Subsidence and Earth Fissures in South-Central and Southern Arizona, USA." *Hydrogeology Journal* 24, no. 3: 649–655. https://doi.org/10.1007/s10040-015-1329-z.

Dodds, W. K., Z. Ratajczak, R. M. Keen, et al. 2023. "Trajectories and State Changes of a Grassland Stream and Riparian Zone After a Decade of Woody Vegetation Removal." *Ecological Applications* 33, no. 4. https://doi.org/10.1002/eap.2830.

Eastoe, C., and D. Towne. 2018. "Regional Zonation of Groundwater Recharge Mechanisms in Alluvial Basins of Arizona: Interpretation of Isotope Mapping." *Journal of Geochemical Exploration* 194: 134–145. https://doi.org/10.1016/j.gexplo.2018.07.013.

Ehleringer, J. R., and T. E. Dawson. 1992. "Water Uptake by Plants: Perspectives From Stable Isotope Composition." *Plant, Cell & Environment* 15, no. 9: 1073–1082. https://doi.org/10.1111/j.1365-3040.1992.tb01657.x.

Ehleringer, J. R., J. Roden, and T. E. Dawson. 2000. "Assessing Ecosystem-Level Water Relations Through Stable Isotope Ratio Analyses." In *Methods in Ecosystem Science*, edited by O. E. Sala, R. B. Jackson, H. A. Mooney, and R. W. Howarth, 181–198. Springer. https://doi.org/10.1007/978-1-4612-1224-9_13.

Ellsworth, P. Z., and D. G. Williams. 2007. "Hydrogen Isotope Fractionation During Water Uptake by Woody Xerophytes." *Plant and Soil* 291, no. 1: 93–107. https://doi.org/10.1007/s11104-006-9177-1.

Gavin, T. A. 1973. "An Ecological Survey of a Mesquite Bosque."

Giordano, C. V., A. Guevara, H. E. Boccalandro, C. Sartor, and P. E. Villagra. 2011. "Water Status, Drought Responses, and Growth of *Prosopis flexuosa* Trees With Different Access to the Water Table in a Warm South American Desert." *Plant Ecology* 212, no. 7: 1123–1134. https://doi.org/10.1007/s11258-010-9892-9.

Glendening, G. E., and H. A. J. Paulsen. 1955. "Reproduction and Establishment of Velvet Mesquite as Related to Invasion of Semidesert Grasslands." Technical Bulletins, Article 156955. https://ideas.repec.org//p/ags/uerstb/156955.html.

Gungle, B., J. B. Callegary, N. V. Paretti, et al. 2016. "Hydrological Conditions and Evaluation of Sustainable Groundwater Use in the Sierra Vista Subwatershed, Upper San Pedro Basin, Southeastern Arizona." In *Scientific Investigations Report (2016–5114)*. U.S. Geological Survey. https://doi.org/10.3133/sir20165114.

Guo, J. S., K. R. Hultine, G. W. Koch, H. Kropp, and K. Ogle. 2020. "Temporal Shifts in Iso/Anisohydry Revealed From Daily Observations of Plant Water Potential in a Dominant Desert Shrub." *New Phytologist* 225, no. 2: 713–726. https://doi.org/10.1111/nph.16196.

Haney, J. 2005. The Lower San Pedro River—Hydrology and Flow Restoration for Biodiversity Conservation. USDA Forest Service Proceedings RMRS-P-36.

Hultine, K. R., D. F. Koepke, W. T. Pockman, A. Fravolini, J. S. Sperry, and D. G. Williams. 2006. "Influence of Soil Texture on Hydraulic Properties and Water Relations of a Dominant Warm-Desert Phreatophyte." *Tree Physiology* 26, no. 3: 313–323. https://doi.org/10.1093/treephys/26.3.313.

Hultine, K. R., R. Froend, D. Blasini, S. E. Bush, M. Karlinski, and D. F. Koepke. 2019. "Hydraulic Traits That Buffer Deep-Rooted Plants From Changes in Hydrology and Climate." *Hydrological Processes* 34, no. 2: 209–222. https://doi.org/10.1002/hyp.13587.

Hultine, K. R., R. L. Scott, W. L. Cable, D. C. Goodrich, and D. G. Williams. 2004. "Hydraulic Redistribution by a Dominant, Warm-Desert Phreatophyte: Seasonal Patterns and Response to Precipitation Pulses." *Functional Ecology* 18, no. 4: 530–538. https://doi.org/10.1111/j.0269-8463.2004.00867.x.

Huxman, T. E., B. P. Wilcox, D. D. Breshears, et al. 2005. "Ecohydrological Implications of Woody Plant Encroachment." *Ecology* 86, no. 2: 308–319. https://doi.org/10.1890/03-0583.

Isaacson, B. N., Y. Yang, M. C. Anderson, K. L. Clark, and J. C. Grabosky. 2023. "The Effects of Forest Composition and Management on Evapotranspiration in the New Jersey Pinelands." *Agricultural and Forest Meteorology* 339: 109588. https://doi.org/10.1016/j.agrformet.2023.109588.

Keen, R. M., J. B. Nippert, P. L. Sullivan, et al. 2022. "Impacts of Riparian and Non-Riparian Woody Encroachment on Tallgrass Prairie Ecohydrology." *Ecosystems* 26, no. 2: 290–301. https://doi.org/10.1007/s10021-022-00756-7.

Kennedy, Jeffrey R., and B. Gungle. 2010. *Quantity and Sources of Base Flow in the San Pedro River Near Tombstone, Arizona*. Scientific Investigations Report. https://doi.org/10.3133/sir20105200.

Lin, G., S. L. Phillips, and J. R. Ehleringer. 1996. "Monosoonal Precipitation Responses of Shrubs in a Cold Desert Community on the Colorado Plateau." *Oecologia* 106, no. 1: 8–17. https://doi.org/10.1007/BF00334402.

McClaran, M. P., and T. R. Van Devender. 1995. *The Desert Grassland*. University of Arizona Press.

Meinzer, F. C., and K. A. McCulloh. 2013. "Xylem Recovery From Drought-Induced Embolism: Where Is the Hydraulic Point of No Return?" *Tree Physiology* 33, no. 4: 331–334. https://doi.org/10.1093/treephys/tpt022.

Minckley, W. L., and T. O. Clark 1984. *Formation and Destruction of a Gila River Mesquite Bosque Community*. CALS Publications Archive. The University of Arizona. https://repository.arizona.edu/handle/10150/552246.

Nilsen, E. T., M. R. Sharifi, and P. W. Rundel. 1991. "Quantitative Phenology of Warm Desert Legumes: Seasonal Growth of Six *Prosopis* Species at the Same Site." *Journal of Arid Environments* 20, no. 3: 299–311. https://doi.org/10.1016/S0140-1963(18)30691-8.

Nilsen, E. T., M. R. Sharifi, P. W. Rundel, W. M. Jarrell, and R. A. Virginia. 1983. "Diurnal and Seasonal Water Relations of the Desert Phreatophyte *Prosopis glandulosa* (Honey Mesquite) in the Sonoran Desert of California." *Ecology* 64, no. 6: 1381–1393. https://doi.org/10.2307/1937492.

Nilsen, E. T., P. W. Rundel, and M. R. Sharifi. 1981. "Summer Water Relations of the Desert Phreatophyte *Prosopis glandulosa* in the Sonoran Desert of Southern California." *Oecologia* 50, no. 2: 271–276. https://doi.org/10.1007/BF00348050.

NOAA. "2022 Monsoon Review." National Weather Service, 11 July 2023, weather.gov/psr/2022MonsoonReview.

O'Keefe, K., D. M. Bell, K. A. McCulloh, and J. B. Nippert. 2020. "Bridging the Flux Gap: Sap Flow Measurements Reveal Species-Specific Patterns of Water Use in a Tallgrass Prairie." *Journal of Geophysical Research: Biogeosciences* 125, no. 2: e2019JG005446. https://doi.org/10.1029/2019JG005446.

OpenET—User Platform. n.d. "OpenET, explore.etdata.org/#15/32.1930/−110.3042." Accessed 9 Oct. 2023.

Pockman, W. T., and J. S. Sperry. 2000. "Vulnerability to Xylem Cavitation and the Distribution of Sonoran Desert Vegetation." *American Journal of Botany* 87, no. 9: 1287–1299. https://doi.org/10.2307/2656722.

Potts, D. L., R. L. Scott, J. M. Cable, T. E. Huxman, and D. G. Williams. 2008. "Sensitivity of Mesquite Shrubland CO2 Exchange to Precipitation in Contrasting Landscape Settings." *Ecology* 89, no. 10: 2900–2910. https://doi.org/10.1890/07-1177.1.

R Core Team 2019. R: A Language and Environment for Statistical Computing R Foundation for Statistical Computing Vienna, Austria https://www.R-project.org/.

Renée Brooks, J., H. R. Barnard, R. Coulombe, and J. J. McDonnell. 2009. "Ecohydrologic Separation of Water Between Trees and Streams in a Mediterranean Climate." *Nature Geoscience* 3, no. 2: 100–104. https://doi.org/10.1038/ngeo722.

Reynolds, J. F., P. R. Kemp, K. Ogle, and R. J. Fernández. 2004. "Modifying the 'Pulse–Reserve' Paradigm for Deserts of North America: Precipitation Pulses, Soil Water, and Plant Responses." *Oecologia* 141, no. 2: 194–210. https://doi.org/10.1007/s00442-004-1524-4.

Sabathier, R., M. B. Singer, J. C. Stella, D. A. Roberts, and K. K. Caylor. 2021. "Vegetation Responses to Climatic and Geologic Controls on Water Availability in Southeastern Arizona." *Environmental Research Letters* 16, no. 6: 064029. https://doi.org/10.1088/1748-9326/abfe8c.

Schenk, H. J., and R. B. Jackson. 2002. "Rooting Depths, Lateral Root Spreads and Below-Ground/Above-Ground Allometries of Plants in Water-Limited Ecosystems." *Journal of Ecology* 90, no. 3: 480–494. https://doi.org/10.1046/j.1365-2745.2002.00682.x.

Scott, R. L., D. Goodrich, L. Levick, et al. 2006. "Determining the Riparian Groundwater Use Within the San Pedro Riparian National Conservation Area and the Sierra Vista Subwatershed, Arizona (Chapter D)." In *Hydrologic Requirements of and Consumptive Ground-Water Use by Riparian Vegetation Along the San Pedro River, Arizona*. Scientific Investigations Report 2005–5163, edited by J. M. Leenhouts, J. C. Stromberg, and R. L. Scott, 107–152. US Geological Survey.

Scott, R. L., T. E. Huxman, D. G. Williams, and D. C. Goodrich. 2006. "Ecohydrological Impacts of Woody-Plant Encroachment: Seasonal Patterns of Water and Carbon Dioxide Exchange Within a Semiarid Riparian Environment." *Global Change Biology* 12, no. 2: 311–324. https://doi.org/10.1111/j.1365-2486.2005.01093.x.

Scott, R. L., W. L. Cable, T. E. Huxman, P. L. Nagler, M. Hernandez, and D. C. Goodrich. 2008. "Multiyear Riparian Evapotranspiration and Groundwater Use for a Semiarid Watershed." *Journal of Arid Environments* 72, no. 7: 1232–1246. https://doi.org/10.1016/j.jaridenv.2008.01.001.

Simonin, K., T. E. Kolb, M. Montes-Helu, and G. W. Koch. 2007. "The Influence of Thinning on Components of Stand Water Balance in a Ponderosa Pine Forest Stand During and After Extreme Drought." *Agricultural and Forest Meteorology* 143, no. 3: 266–276. https://doi.org/10.1016/j.agrformet.2007.01.003.

Snyder, K. A., and D. G. Williams. 2007. "Root Allocation and Water Uptake Patterns in Riparian Tree Saplings: Responses to Irrigation and Defoliation." *Forest Ecology and Management* 246, no. 2–3: 222–231. https://doi.org/10.1016/j.foreco.2007.04.032.

Snyder, K., and D. G. Williams. 2000. "Water Sources Used by Riparian Trees Varies Among Stream Types on the San Pedro River, Arizona." *Agricultural and Forest Meteorology* 105, no. 1–3: 227–240. https://doi.org/10.1016/S0168-1923(00)00193-3.

Stromberg, J. C. 1993. "Riparian Mesquite Forests: A Review of Their Ecology, Threats, and Recovery Potential."

Stromberg, J. C. 2001. "Restoration of Riparian Vegetation in the South-Western United States: Importance of Flow Regimes and Fluvial Dynamism." *Journal of Arid Environments* 49, no. 1: 17–34. https://doi.org/10.1006/jare.2001.0833.

Stromberg, J. C., J. A. Tress, S. D. Wilkins, and S. D. Clark. 1992. "Response of Velvet Mesquite to Groundwater Decline." *Journal of Arid Environments* 23, no. 1: 45–58. https://doi.org/10.1016/S0140-1963(18)30540-8.

Stromberg, J. C., S. D. Wilkins, and J. A. Tress. 1993. "Vegetation-Hydrology Models: Implications for Management of *Prosopis velutina* (Velvet Mesquite) Riparian Ecosystems." *Ecological Applications* 3, no. 2: 307–314. https://doi.org/10.2307/1941833.

West, A. G., G. R. Goldsmith, P. D. Brooks, and T. E. Dawson. 2010. "Discrepancies Between Isotope Ratio Infrared Spectroscopy and Isotope Ratio Mass Spectrometry for the Stable Isotope Analysis of Plant and Soil Waters." *Rapid Communications in Mass Spectrometry* 24, no. 14: 1948–1954. https://doi.org/10.1002/rcm.4597.

Wilcox, B. P. 2002. Shrub Control and Streamflow on Rangelands: A Process Based Viewpoint. 55. https://doi.org/10.2458/azu_jrm_v55i4_wilcox.

Wilcox, B. P., M. K. Owens, W. A. Dugas, D. N. Ueckert, and C. R. Hart. 2006. "Shrubs, Streamflow, and the Paradox of Scale." *Hydrological Processes* 20, no. 15: 3245–3259. https://doi.org/10.1002/hyp.6330.

Wu, X., M. Pan, J. Yin, and J. Cao. 2023. "Hydrogen and Oxygen Isotope Signal Transmission in Rainfall, Soil Water, and Cave Drip Water in Liangfeng Cave, Southwest China." *Applied Geochemistry* 158: 105798. https://doi.org/10.1016/j.apgeochem.2023.105798.

Zimmermann, R. C. 1969. Plant Ecology of an Arid Basin, Tres Alamos-Redington Area, Southeastern Arizona. In Professional Paper (485-D). U.S. Govt. Print. Off. https://doi.org/10.3133/pp485D.

Supporting Information

Additional supporting information can be found online in the Supporting Information section. **Figure S1:** Oxygen ($\delta^{18}O$) and hydrogen ($\delta^{2}H$) isotopes from tree xylem for the old-growth (OG) study area. Plots bordered in blue indicate sample dates during the monsoon rain season. Precipitation is also plotted on the local meteoric water line. **Figure S2:** Oxygen ($\delta^{18}O$) and hydrogen ($\delta^{2}H$) isotopes from tree xylem for the dense thicket (DT) study area. Plots bordered in blue indicate sample dates during the monsoon rain season. Precipitation is also plotted on the local meteoric water line. **Figure S3:** Oxygen ($\delta^{18}O$) and hydrogen ($\delta^{2}H$) isotopes from tree xylem for the Thinned thicket (TT) study area. Plots bordered in blue indicate sample dates during the monsoon rain season. Precipitation is also plotted on the local meteoric water line. **Figure S4:** Oxygen ($\delta^{18}O$) and hydrogen ($\delta^{2}H$) isotopes from tree xylem for the Upland (UL) study area. Plots bordered in blue indicate sample dates during the monsoon rain season. Precipitation is also plotted on the local meteoric water line. **Figure S5:** Ψleaf (leaf water potential) during summer of 2022 and 2023 for individual trees at the old-growth (OG) study plot. Blue boxes indicate months with monsoon rainfall. **Figure S6:** Ψleaf (leaf water potential) during summer of 2022 and 2023 for individual trees at the dense thicket (DT) study plot. Blue boxes indicate months with monsoon rainfall. **Figure S7:** Ψleaf (leaf water potential) during summer of 2022 and 2023 for individual trees at the thinned thicket (TT) study plot. Blue boxes indicate months with monsoon rainfall.